SCIENCE CHINA
Physics, Mechanics & Astronomy

• Invited Review •

April 2018 Vol. 61 No. 4: 049501
https://doi.org/10.1007/s11433-017-9142-2

Neutrinos, supernovae, and the origin of the heavy elements

YongZhong Qian[1,2*]

[1] *School of Physics and Astronomy, University of Minnesota, Minneapolis 55455, USA;*
[2] *Tsung-Dao Lee Institute, Shanghai 200240, China*

Received October 23, 2017; accepted November 29, 2017; published online January 22, 2018

Stars of ~ 8-100 $M_\odot$ end their lives as core-collapse supernovae (SNe). In the process they emit a powerful burst of neutrinos, produce a variety of elements, and leave behind either a neutron star or a black hole. The wide mass range for SN progenitors results in diverse neutrino signals, explosion energies, and nucleosynthesis products. A major mechanism to produce nuclei heavier than iron is rapid neutron capture, or the *r* process. This process may be connected to SNe in several ways. A brief review is presented on current understanding of neutrino emission, explosion, and nucleosynthesis of SNe.

neutrino, supernova, nucleosynthesis, the *r* process

PACS number(s): 26.30.Jk, 26.30.Hj, 97.60.Bw, 14.60.Pq

Citation: Y. Z. Qian, Neutrinos, supernovae, and the origin of the heavy elements, Sci. China-Phys. Mech. Astron. **61**, 049501 (2018), https://doi.org/10.1007/s11433-017-9142-2

1 Introduction

After baryogenesis in the early universe and when the temperature drops to $T \sim 100$ MeV, the only baryons present are neutrons and protons. Because matter at such a high temperature is in thermal equilibrium, the neutron-to-proton ratio n/p is determined by their mass difference $\Delta = m_n - m_p = 1.293$ MeV through the Boltzmann factor:

$$n/p = \exp(-\Delta/T). \quad (1)$$

It is a remarkable achievement of the standard model of particle physics that this mass difference can now be calculated from first principles to within 20% [1]. Because a neutron is heavier than a proton, the equilibrium abundance shifts more and more towards protons as T drops. This shift is accomplished by the competition among the weak interactions interconverting neutrons and protons:

$$\nu_e + n \rightleftharpoons p + e^-, \quad (2)$$

$$\bar{\nu}_e + p \rightleftharpoons n + e^+. \quad (3)$$

Because the rates of these interactions also decrease with T, the neutron-to-proton ratio eventually freezes out at $T \sim 1$ MeV. As the universe cools further, big bang nucleosynthesis fuses neutrons and protons into light nuclei such as ^{2}H, ^{3}H, ^{3}He, ^{4}He, ^{7}Li, and ^{7}Be.

Under the influence of gravity, big bang debris containing mostly protons condenses into stars, which shine by burning protons into heavier nuclei and provide the newly-synthesized products to the interstellar medium when they die. Therefore, the next generation of stars formed from this medium are enriched beyond the big bang composition. This cycle repeats as generation after generation of stars are born, lead luminous lives, die glorious deaths, and in the process convert primordial baryons into nuclei of the entire periodic table. To quantify this picture of cosmic alchemy, we can compare the composition of big bang debris with that in the sun, which formed ≈ 9 Gyr after the big bang. The dominant

*Corresponding author (email: qian@physics.umn.edu)

products of big bang nucleosynthesis are protons and ^{4}He with mass fractions of $\approx 75\%$ and $\approx 25\%$, respectively. The mass fractions of protons, ^{4}He, and nuclei for the rest of the elements in the sun are $\approx 71.1\%$, $\approx 27.4\%$, and $\approx 1.5\%$, respectively. Clearly, the net effect of stellar processing is to convert protons into nuclei containing both protons and neutrons. Although the actual processes involve many steps, we can state in general that this end result must be achieved with the help of weak interactions of the following types:

$$(Z, N) \rightarrow (Z-1, N+1) + e^+ + \nu_e, \quad (4)$$

$$e^- + (Z, N) \rightarrow (Z-1, N+1) + \nu_e, \quad (5)$$

$$\bar{\nu}_e + (Z, N) \rightarrow (Z-1, N+1) + e^+, \quad (6)$$

where (Z, N) indicates a nucleus with Z protons and N neutrons.

The following examples serve to illustrate the critical roles of the above weak interactions in providing neutrons for making nuclei. The β^+ decay of ^{13}N is of the type in eq. (4) and is the crucial step in the reaction sequence $^{12}\mathrm{C}(p,\gamma)^{13}\mathrm{N}(e^+\nu_e)^{13}\mathrm{C}(\alpha,n)^{16}\mathrm{O}$ that provides a major neutron source for *s*-process nucleosynthesis in stars of $\sim$ 1-3 $M_\odot$ (see e.g., ref. [2] for a review). The reverse reaction in eq. (2) is of the type in eq. (5) and is responsible for converting the Fe core of a massive ($\gtrsim 8\,M_\odot$) star into a neutron star (NS). If the NS is formed in a binary with another NS or a black hole (BH) as its companion, then it can be tapped as a powerful neutron source for *r*-process nucleosynthesis through its disruption during the merger with its companion (see sect. 2.5). The forward reaction in eq. (3) is of the type in eq. (6) and plays an important role in supernova nucleosynthesis (see sect. 2.3). The above discussion shows that neutrinos are intimately associated with the origin of the elements.

2 The *r* process and supernovae

Before further discussing the roles of neutrinos in nucleosynthesis, we first describe how heavy nuclei are made by capturing neutrons. There are two prominent sets of peaks in the abundance distribution of nuclei heavier than Fe in the solar system. One set contains nuclei such as ^{138}Ba and ^{208}Pb with magic neutron numbers 82 and 126, respectively. These are produced by the so-called slow neutron-capture (*s*) process. Once stable nuclei with magic neutron numbers are produced by the *s* process, they are hard to destroy due to their small neutron-capture cross sections. So they pile up and form peaks. In contrast to the *s* process whose path stays close to stable nuclei, the so-called rapid neutron-capture (*r*) process initially produces nuclei far from stability. This is because the neutron density in the *r*-process environment is so high that neutron capture on the unstable nuclei produced occurs much faster than their β decay. Unstable nuclei with magic neutron numbers also form peaks because they are relatively more stable. On exhaustion of neutrons, these nuclei β decay to stability and give rise to the peaks at mass numbers $A \sim 130$ and 195, respectively, in the solar abundance distribution.

The *r* process (see e.g., refs. [3-6] for reviews) has a lot to do with the death of a massive star in a core-collapse supernova (SN). The connection between such an SN and the formation of an NS was proposed by Baade and Zwicky [7] shortly after the discovery of the neutron by Chadwick in 1932. They observed an extremely bright SN and found that the net energy of radiation was enormous [8]. They also found that a comparable amount of energy from each past SN could power the cosmic rays [7]. To account for the required energy in each case, they made the following proposal [7]. "With all reserve we advance the view that a super-nova represents the transition of an ordinary star into a neutron star, consisting mainly of neutrons. Such a star may possess a very small radius and an extremely high density. As neutrons can be packed much more closely than ordinary nuclei and electrons, the 'gravitational packing' energy in a cold neutron star may become very large, and under certain circumstances, may far exceed the ordinary nuclear packing fractions."

We now know that the total amount of energy emitted in photons by a typical SN is $\sim 10^{49}$ ergs and the kinetic energy of the SN debris is $\sim 10^{51}$ ergs. By comparison, the gravitational binding energy $E_{\rm G}$ of an NS is

$$E_{\rm G} \sim \frac{3}{5}\frac{GM_{\rm NS}^2}{R_{\rm NS}} \sim 3\times 10^{53}\left(\frac{M_{\rm NS}}{1.4M_\odot}\right)^2\left(\frac{10\ {\rm km}}{R_{\rm NS}}\right)\ {\rm ergs}, \quad (7)$$

where nominal values of the NS mass $M_{\rm NS}$ and radius $R_{\rm NS}$ are indicated. Although Baade and Zwicky did not give an explicit estimate of $E_{\rm G}$, which they referred to as the "gravitational packing" energy, they correctly suggested that this energy may far exceed the binding energy released in nuclear reactions, which they meant by "ordinary nuclear packing fractions." Indeed, $E_{\rm G}$ corresponds to $\sim$ 100 MeV/nucleon, which is much higher than the typical nuclear binding energy of $\sim$ 8 MeV/nucleon. Furthermore, the insightful association of NS formation and cosmic-ray production with SNe by Baade and Zwicky has been put on much firmer grounds.

2.1 SN explosion

Only massive stars of $\gtrsim 8\,M_\odot$ can become SNe. A star of $\sim$ 8-9 $M_\odot$ develops an O-Ne-Mg core at the end of its life. The density in the core is so high that the electrons there are relativistically degenerate. Capture of these electrons by Ne and Mg nuclei reduces the electron degeneracy pressure and triggers the collapse of the core. In con-

trast, a star of $> 9\,M_\odot$ develops an Fe core, which collapses when thermal energy is lost due to photo-dissociation of Fe-group nuclei. In both cases, the inner core bounces due to the repulsive nuclear force at very short range when supra-nuclear density is reached. This bounce launches a shock wave into the still-collapsing outer core. However, the shock quickly loses energy on its way out by dissociating nuclei into free nucleons and is stalled before exiting the outer core. The inner core is now a proto-NS and material falling onto it releases the gravitational binding energy by emitting mostly ν_e and $\bar{\nu}_e$. Some of these ν_e and $\bar{\nu}_e$ are captured by neutrons and protons through the forward reactions in eqs. (2) and (3), respectively, to heat the material behind the stalled shock. In some cases, this neutrino heating provides sufficient energy to revive the shock, which proceeds to make an explosion. This is the so-called neutrino-driven SN mechanism [9].

The above SN mechanism has been consistently demonstrated by several groups for a star of $8.8\,M_\odot$ [10-12]. However, the same mechanism is harder to operate in more massive stars, which have more extended envelopes with larger gravitational binding energies. For these more massive stars, the shock is required to do extra work and sometimes neutrinos fail to deliver an explosion. At the present time, whether neutrino-driven explosion works for stars of $> 9\,M_\odot$ and if so, how exactly it works are under intense study by many SN modelers around the world [13]. An exploratory study by the Garching group in Germany found that whether neutrino-driven explosion works is not a simple function of the SN progenitor mass [13]. In addition, when a neutrino-driven SN occurs, it takes $\sim$ 0.1 to $\sim$ 1 s and the explosion energy varies from $\sim 10^{50}$ to $\sim 10^{51}$ ergs. Neither the time nor the energy of explosion is a monotonic function of the progenitor mass.

A successful explosion typically leaves behind an NS of a few $M_\odot$, while a failed SN produces a BH that swallows the entire progenitor star most of the time. In some cases, an accretion disk may form around the BH and powers a jet that drives an explosion ejecting part of the progenitor star. In rare cases, this jet-driven mechanism gives rise to the so-called hypernovae associated with long gamma-ray bursts [14].

2.2 SN neutrino emission

The ν_e and $\bar{\nu}_e$ potentially driving the explosion are emitted dominantly through the reverse reactions in eqs. (2) and (3), respectively, by material falling onto the proto-NS. The so-called accretion phase associated with this emission lasts $\sim$ 0.1 to $\sim$ 1 s. The gravitational binding energy of the proto-NS itself [7] is released in ν_e, $\bar{\nu}_e$, ν_μ, $\bar{\nu}_\mu$, ν_τ, and $\bar{\nu}_\tau$ during the so-called cooling phase, for which the important neutrino production mechanisms are processes such as $e^+ + e^- \rightarrow \nu + \bar{\nu}$. The cooling phase lasts $\sim$ 10 s because neutrinos must diffuse out of the extremely hot and dense interior of the proto-NS. Detection of the neutrino burst from SN 1987A [15,16], which lasted $\sim$ 13 s, confirmed this overall picture of SN neutrino emission.

The characteristics of neutrino emission differ greatly between the accretion and cooling phases. Figure 1 shows the evolution of neutrino luminosities and average neutrino energies as functions of time for an $18\,M_\odot$ SN model [12,17]. During the accretion phase (Figure 1(b), time post core bounce $t_{\rm pb} \sim$ 0.05-0.6 s), the $\bar{\nu}_e$ luminosity $L_{\bar{\nu}_e}$ is approximately the same as the ν_e luminosity L_{ν_e}. Both follow nearly the same time evolution and are much higher than the luminosity $L_{\nu_x} \approx L_{\bar{\nu}_x}$ ($x = \mu, \tau$) of any other species. In addition, the average neutrino energies (Figure 1(e)) follow a clear hierarchy $\langle E_{\nu_e}\rangle < \langle E_{\bar{\nu}_e}\rangle < \langle E_{\nu_x}\rangle \approx \langle E_{\bar{\nu}_x}\rangle$, with $\langle E_{\nu_e}\rangle \approx$ 8-11 MeV, $\langle E_{\bar{\nu}_e}\rangle \approx$ 11-12 MeV, and $\langle E_{\nu_x}\rangle \approx \langle E_{\bar{\nu}_x}\rangle \approx$ 16-14 MeV. In contrast, $L_{\nu_x} \approx L_{\bar{\nu}_x}$ is close to $L_{\nu_e} \approx L_{\bar{\nu}_e}$ during the cooling phase (Figure 1(c), $t_{\rm pb} > 0.6$ s), with all species having nearly the same luminosity eventually. The average neutrino energies monotonically decrease with time (Figure 1(f)), and also become less distinctive from each other. While $\langle E_{\nu_e}\rangle$ remains the lowest, the difference between $\langle E_{\bar{\nu}_e}\rangle$ and $\langle E_{\nu_x}\rangle \approx \langle E_{\bar{\nu}_x}\rangle$ becomes smaller and smaller. Note that Figure 1(a) and (d) correspond to the so-called shock-breakout phase. As the shock breaks through the neutrino-trapping surface formed by nuclei of the Fe group, the protons released from the dissociation of these nuclei rapidly capture

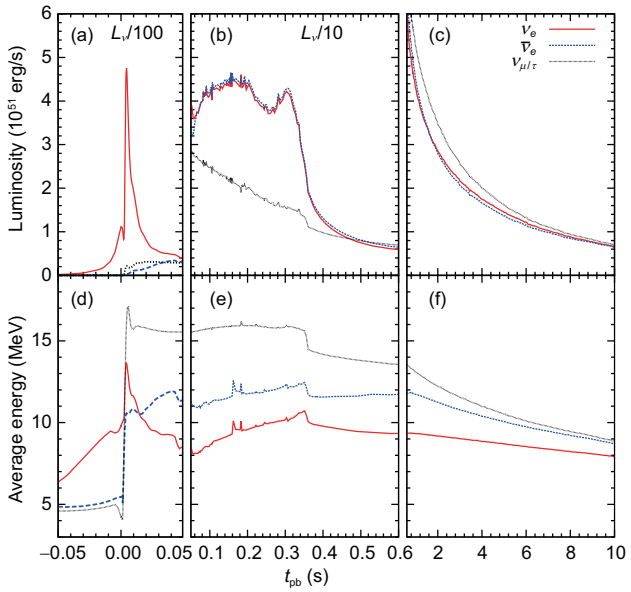

Figure 1 (Color online) Evolution of neutrino luminosities and average neutrino energies as functions of time for an $18\,M_\odot$ SN model [12,17]. (a) and (d) correspond to the shock-breakout phase, (b) and (e) correspond to the accretion phase, and (c) and (f) correspond to the cooling phase [17].

electrons to produce a strong ν_e pulse. Therefore, the shock-breakout phase is characterized by powerful emission of predominantly ν_e.

For SNe with different progenitors, the shock-breakout pulse is a common feature that signifies the launch of the prompt shock. A ν_e pulse with $L_{\nu_e} \approx$ (4-5) $\times 10^{53}$ erg/s and a width of $\sim$ 10 ms is typical of all SNe. For those SNe with neutrino-driven explosion, the duration of the accretion phase depends on the progenitor. For example, this phase lasts $\sim$ 0.6 s for the 18 $M_\odot$ model described above, which is $\sim$ 3 times longer than that for the 8.8 $M_\odot$ model discussed in ref. [13]. The cooling phase is similar for all SNe that leave behind NS remnants. For SNe producing BHs, when the BH forms depends on the progenitor structure and the nuclear equation of state. If a BH forms during the first $\sim$ 10 s after core bounce, neutrino emission from the proto-NS is abruptly terminated (e.g., ref. [18]). However, if there is an accretion disk surrounding the BH, significant neutrino emission from this disk might continue for some time (e.g., ref. [19]).

2.3 Neutrino-driven winds and heavy-element synthesis

Subsequent to a successful SN explosion, material in the vicinity of the proto-NS is still heated by ν_e and $\bar{\nu}_e$ through the forward reactions in eqs. (2) and (3), respectively. When this material acquires sufficient energy from neutrino heating, it overcomes the gravitational potential of the proto-NS and escapes as the so-called neutrino-driven wind. The neutron-to-proton ratio in the wind is determined by the competition between neutron production by $\bar{\nu}_e$ and proton production by ν_e through the same reactions that provide the heating [20, 21]. The rates for these reactions at radius r are

$$\lambda_{\bar{\nu}_e p} = \frac{L_{\bar{\nu}_e}}{4\pi r^2}\frac{\langle\sigma_{\bar{\nu}_e p}\rangle}{\langle E_{\bar{\nu}_e}\rangle} \propto L_{\bar{\nu}_e}\left(\frac{\langle E^2_{\bar{\nu}_e}\rangle}{\langle E_{\bar{\nu}_e}\rangle} - 2\Delta\right), \tag{8}$$

$$\lambda_{\nu_e n} = \frac{L_{\nu_e}}{4\pi r^2}\frac{\langle\sigma_{\nu_e n}\rangle}{\langle E_{\nu_e}\rangle} \propto L_{\nu_e}\left(\frac{\langle E^2_{\nu_e}\rangle}{\langle E_{\nu_e}\rangle} + 2\Delta\right), \tag{9}$$

where the angular brackets indicate averaging over the relevant neutrino energy spectrum, $\sigma_{\bar{\nu}_e p} \propto (E_{\bar{\nu}_e} - \Delta)^2$ and $\sigma_{\nu_e n} \propto (E_{\nu_e} + \Delta)^2$ are the cross sections for the corresponding reactions, and we have ignored terms proportional to Δ^2. The neutron-to-proton ratio in the wind can be estimated as:

$$n/p \approx \frac{\lambda_{\bar{\nu}_e p}}{\lambda_{\nu_e n}} \approx \frac{L_{\bar{\nu}_e}}{L_{\nu_e}}\left(\frac{\epsilon_{\bar{\nu}_e} - 2\Delta}{\epsilon_{\nu_e} + 2\Delta}\right), \tag{10}$$

where $\epsilon_\nu \equiv \langle E^2_\nu\rangle/\langle E_\nu\rangle$. For $L_{\bar{\nu}_e} \approx L_{\nu_e}$, $n/p > 1$ requires $\epsilon_{\bar{\nu}_e} - \epsilon_{\nu_e} > 4\Delta$.

Because neutrino energy spectra are determined by neutrino opacities in the surface layers of the proto-NS, whether the wind is neutron rich is sensitive to neutrino interactions in hot and dense matter. Using various approximate neutrino opacities, earlier studies found the wind to be mostly neutron rich (e.g., ref. [21, 22]), whereas later ones obtained only proton-rich winds (e.g., ref. [23]) with neutrino emission parameters similar to those shown in Figure 1. Recently, two groups [24, 25] studied ν_e and $\bar{\nu}_e$ opacities in some detail and found that the wind may be neutron rich for a significant period of time.

A number of groups (e.g., refs. [21, 22, 26-31]) have studied other conditions such as the entropy and expansion timescale in the neutrino-driven wind and surveyed the resulting nucleosynthesis. The general consensus is that elements such as Sr, Y, and Zr with $A \sim 90$ can be readily produced for somewhat neutron-rich winds. It is likely that the production can be extended to Pd and Ag with $A \sim 110$. However, these nuclei are made mainly through a quasi-equilibrium process [32] involving (n,γ), (p,γ), (n,p), (α,γ), (α,n), (α,p), and their reverse reactions, in contrast to the classical r process where neutron capture plays a dominant role. With extreme conditions such as associated with a massive proto-NS [33], a classical r process can occur to produce nuclei up to $A \sim 130$. However, it is very difficult to justify conditions for making r-process nuclei with $A \sim 195$ in the wind.

2.4 Neutrino-induced *r* process in helium shells

In addition to driving a neutron-rich wind, neutrino interactions in SNe can provide neutrons in other ways as well. For example, neutral-current reactions on ^{4}He nuclei can produce neutrons through $^4\mathrm{He}(\nu,\nu n)^3\mathrm{He}(n,p)^3\mathrm{H}$ and $^4\mathrm{He}(\nu,\nu p)^3\mathrm{H}$ followed by $^3\mathrm{H}(^3\mathrm{H},2n)^4\mathrm{He}$. In the helium (He) shell of an early SN, these neutrons are captured by the few ^{56}Fe nuclei present in the birth material of the progenitor, but not by the predominant ^{4}He nuclei. This scenario was proposed as a model for the r process [34]. It was critically examined by ref. [35], which constrained it to be viable only for some special metal-poor SNe with He shells at very small radii and hence, exposed to large neutrino fluxes for neutron production.

A recent study [36] reexamined the above scenario for a neutrino-induced r process. Using updated models of metal-poor massive stars, it found that the ^{3}H nuclei produced by neutral-current neutrino reactions on ^{4}He lead to production of ^{7}Li through $^4\mathrm{He}(^3\mathrm{H},\gamma)^7\mathrm{Li}$ instead of generating neutrons as in the original scenario. However, the charged-current reaction

$$\bar{\nu}_e + {}^4\mathrm{He} \rightarrow {}^3\mathrm{H} + n + e^+ \tag{11}$$

may provide a new neutron source, especially in the presence of $\bar{\nu}_e \rightleftharpoons \bar{\nu}_x$ oscillations. The reaction in eq. (11) has a thresh-

old of 21.6 MeV, which is significantly above the average $\bar{\nu}_e$ energy in the absence of flavor oscillations. Earlier SN neutrino transport calculations (e.g., ref. [22]) gave a very hard $\bar{\nu}_x$ spectrum with $\langle E_{\bar{\nu}_x}\rangle \sim$ 20-25 MeV. More recent calculations also showed that the emission spectrum of $\bar{\nu}_x$ is significantly harder than that of $\bar{\nu}_e$ at least for a few seconds (Figure 1). For an inverted neutrino mass hierarchy, $\bar{\nu}_e \rightleftharpoons \bar{\nu}_x$ oscillations can occur before neutrinos reach the He shell, thereby giving rise to a harder effective $\bar{\nu}_e$ spectrum for neutron production.

The neutron production rate per ^{4}He nucleus is

$$\lambda_{\bar{\nu}_e\alpha,n} = \frac{1}{4\pi r^2}\left[\frac{L_{\bar{\nu}_e}\langle\sigma_{\bar{\nu}_e\alpha,n}\rangle}{\langle E_{\bar{\nu}_e}\rangle}\right]_{\rm eff} \propto \frac{(L_{\bar{\nu}_e}T^p_{\bar{\nu}_e})_{\rm eff}}{r^2}, \quad (12)$$

where $\langle\sigma_{\bar{\nu}_e\alpha,n}\rangle$ is the cross section for the charged-current reaction in eq. (11) averaged over the $\bar{\nu}_e$ spectrum, the subscript "eff" denotes effective quantities for $\bar{\nu}_e$ in the presence of $\bar{\nu}_e \rightleftharpoons \bar{\nu}_x$ oscillations, $T_{\bar{\nu}_e}$ is the temperature for a Fermi-Dirac spectrum with zero chemical potential, and the power index p is $\sim$ 5-6. Using the neutrino emission spectra of ref. [22] and invoking $\bar{\nu}_e \rightleftharpoons \bar{\nu}_x$ oscillations, ref. [36] showed that an r process can occur and produce nuclei up to $A > 200$ in the He shell of an 11 $M_\odot$ SN model with an initial metallicity of [Fe/H] $\equiv \log(\mathrm{Fe/H}) - \log(\mathrm{Fe/H})_\odot \sim -4.5$.

The neutron density obtained in the He shell is approximately determined by the competition between neutrino-induced production and capture by nuclei such as ^{56}Fe in the birth material. As the metallicity of the SN progenitor increases, more ^{56}Fe nuclei are available to capture neutrons, which results in lower neutron densities and less efficient production of nuclei heavier than ^{56}Fe. Consequently, the above neutrino-induced r process ceases to operate at [Fe/H] $\gtrsim -3$. This dependence on metallicity [37] is illustrated in Figure 2.

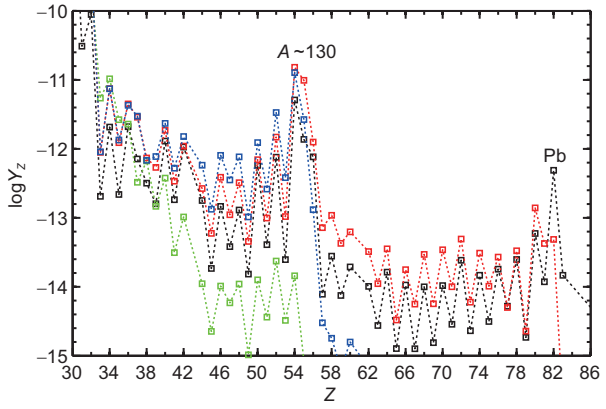

Figure 2 (Color online) Effect of SN progenitor metallicity on neutrino-induced r-process nucleosynthesis in He shells [36, 37]. Final elemental abundance patterns are shown as functions of atomic number Z for 11 $M_\odot$ models with metallicities of [Fe/H] ~ -5 (black), -4 (red and blue), and -3 (green). The two models with [Fe/H] ~ -4 have different abundances of ^{28}S and ^{32}Si in the He shell ($\sim$ 10 times smaller for the red curve [37]).

2.5 NS mergers and the *r* process

The NS left behind by an SN is a great source of neutron-rich material. This source can be tapped to drive a robust r process during mergers of an NS with another NS or a BH. The progenitor system of such a merger is a binary consisting of two massive stars, which explode as SNe without disrupting the system. Energy loss through radiation of gravitational waves leads to the eventual merger of the two compact remnants left by the SNe. Pioneering work on r-process nucleosynthesis during decompression of cold NS matter was carried out in ref. [38]. More recently, detailed hydrodynamic simulations of an NS-NS merger were performed (e.g., refs. [39, 40]). It was shown that r-process nuclei with $A \gtrsim 130$ including thorium and uranium are produced in the extremely neutron-rich ejecta. In addition, the less neutron-rich material ejected from the accretion disk surrounding the merger remnant has similar nucleosynthesis (e.g., ref. [41]) to the neutron-rich neutrino-driven winds from a proto-NS (see sect. 2.3).

The production of r-process nuclei with $A \gtrsim 130$ and the associated production of lighter nuclei in an NS-NS merger received strong support from the observations of such an event, GW170817, through gravitational waves [42] and electromagnetic radiation. In this regard, the most dramatic observation of this event is the detection of the so-called kilonova [43], which was powered by the decay of the nuclei synthesized by the r process (e.g., ref. [44]).

3 Conclusion

Eight decades after Baade and Zwicky proposed the connection between SNe and NS formation, we are still figuring out the mechanisms through which SNe occur. It has been shown that neutrino-driven explosion works for stars of $\sim$ 8-9 $M_\odot$. While neutrinos may also play important roles in explosions of more massive stars, the detailed mechanisms in these cases are rather uncertain but under intense investigation at the present time. Nevertheless, it appears that SNe from stars of $\sim$ 8-100 $M_\odot$ have a wide range of neutrino signals, explosion energies, nucleosynthesis products, and compact remnant (NS or BH) masses.

With formation of an NS and the associated profuse emission of neutrinos, SNe can provide neutrons for making heavy nuclei, especially through the r process, in several ways. First of all, neutrino-driven winds from a proto-NS can be neutron rich due to the dominance of the forward reaction in eq. (3). These winds can produce elements from Sr, Y, Zr ($A \sim 90$) up to Pd and Ag ($A \sim 110$) through a quasi-equilibrium process, and for the most favorable conditions, make nuclei up to $A \sim 130$ through the r process. In addition, $\bar{\nu}_e$ can produce

neutrons through the reaction in eq. (11). This may give rise to a neutrino-induced *r* process in the He shell of an early SN where neutrons are captured by the few ^{56}Fe nuclei present in the birth material of the progenitor star. As neutron production is sensitive to the effective $\bar{\nu}_e$ energy spectrum in the He shell, this neutrino-induced *r* process can be enhanced greatly by $\bar{\nu}_e \rightleftharpoons \bar{\nu}_x$ oscillations, the occurrence of which most likely requires an inverted neutrino mass hierarchy. In the optimal case, nuclei with $A > 200$ can be produced. However, the neutrino-induced *r* process ceases to operate when metallicities of SN progenitors exceed [Fe/H] ~ -3. Finally, a small fraction of binary systems consisting of two massive stars can evolve into NS-NS or NS-BH binaries after surviving two SNe. Cold NS matter ejected from mergers of the two compact remnants in such binaries serves as the best site for making *r*-process nuclei with $A \gtrsim 130$ including thorium and uranium.

This work was supported by the US Department of Energy (Grant No. DE-FG02-87ER40328). I thank Projjwal Banerjee, Tobias Fischer, Wick Haxton, Alexander Heger, Gabriel Martínez-Pinedo, and Meng-Ru Wu for fruitful collaboration.

1 S. Borsanyi, S. Durr, Z. Fodor, C. Hoelbling, S. D. Katz, S. Krieg, L. Lellouch, T. Lippert, A. Portelli, K. K. Szabo, and B. C. Toth, Science **347**, 1452 (2015).
2 F. Käppeler, R. Gallino, S. Bisterzo, and W. Aoki, Rev. Mod. Phys. **83**, 157 (2011).
3 Y. Z. Qian, Prog. Particle Nucl. Phys. **50**, 153 (2003).
4 Y. Qian, and G. Wasserburg, Phys. Rep. **442**, 237 (2007).
5 M. Arnould, S. Goriely, and K. Takahashi, Phys. Rep. **450**, 97 (2007).
6 Y. Z. Qian, J. Phys. G-Nucl. Part. Phys. **41**, 044002 (2014).
7 W. Baade, and F. Zwicky, Proc. Natl. Acad. Sci. USA **20**, 259 (1934).
8 W. Baade, and F. Zwicky, Proc. Natl. Acad. Sci. USA **20**, 254 (1934).
9 H. A. Bethe, and J. R. Wilson, Astrophys. J. **295**, 14 (1985).
10 R. Mayle, and J. R. Wilson, Astrophys. J. **334**, 909 (1988).
11 F. S. Kitaura, H. T. Janka, and W. Hillebrandt, Astron. Astrophys. **450**, 345 (2006).
12 T. Fischer, S. C. Whitehouse, A. Mezzacappa, F. K. Thielemann, and M. Liebendörfer, Astron. Astrophys. **517**, A80 (2010).
13 H. T. Janka, Annu. Rev. Nucl. Part. Sci. **62**, 407 (2012).
14 A. I. MacFadyen, and S. E. Woosley, Astrophys. J. **524**, 262 (1999).
15 K. Hirata, T. Kajita, M. Koshiba, M. Nakahata, Y. Oyama, N. Sato, A. Suzuki, M. Takita, Y. Totsuka, T. Kifune, T. Suda, K. Takahashi, T. Tanimori, K. Miyano, M. Yamada, E. W. Beier, L. R. Feldscher, S. B. Kim, A. K. Mann, F. M. Newcomer, R. Van, W. Zhang, and B. G. Cortez, Phys. Rev. Lett. **58**, 1490 (1987).
16 R. M. Bionta, G. Blewitt, C. B. Bratton, D. Casper, A. Ciocio, R. Claus, B. Cortez, M. Crouch, S. T. Dye, S. Errede, G. W. Foster, W. Gajewski, K. S. Ganezer, M. Goldhaber, T. J. Haines, T. W. Jones, D. Kielczewska, W. R. Kropp, J. G. Learned, J. M. LoSecco, J. Matthews, R. Miller, M. S. Mudan, H. S. Park, L. R. Price, F. Reines, J. Schultz, S. Seidel, E. Shumard, D. Sinclair, H. W. Sobel, J. L. Stone, L. R. Sulak, R. Svoboda, G. Thornton, J. C. van der Velde, and C. Wuest, Phys. Rev. Lett. **58**, 1494 (1987).
17 M. R. Wu, Y. Z. Qian, G. Martínez-Pinedo, T. Fischer, and L. Huther, Phys. Rev. D **91**, 065016 (2015).
18 T. Fischer, S. C. Whitehouse, A. Mezzacappa, F. K. Thielemann, and M. Liebendoörfer, Astron. Astrophys. **499**, 1 (2009).
19 R. Popham, S. E. Woosley, and C. Fryer, Astrophys. J. **518**, 356 (1999).
20 Y. Z. Qian, G. M. Fuller, G. J. Mathews, R. W. Mayle, J. R. Wilson, and S. E. Woosley, Phys. Rev. Lett. **71**, 1965 (1993).
21 Y. Z. Qian, and S. E. Woosley, Astrophys. J. **471**, 331 (1996).
22 S. E. Woosley, J. R. Wilson, G. J. Mathews, R. D. Hoffman, and B. S. Meyer, Astrophys. J. **433**, 229 (1994).
23 L. Hüdepohl, B. Müller, H. T. Janka, A. Marek, and G. G. Raffelt, Phys. Rev. Lett. **104**, 251101 (2010).
24 G. Martínez-Pinedo, T. Fischer, A. Lohs, and L. Huther, Phys. Rev. Lett. **109**, 251104 (2012).
25 L. F. Roberts, S. Reddy, and G. Shen, Phys. Rev. C **86**, 065803 (2012).
26 J. Witti, H. T. Janka, and K. Takahashi, Astron. Astrophys. **286**, 841 (1994).
27 J. Witti, H. T. Janka, and K. Takahashi, Astron. Astrophys. **286**, 857 (1994).
28 R. D. Hoffman, S. E. Woosley, and Y. Z. Qian, Astrophys. J. **482**, 951 (1997).
29 S. Wanajo, T. Kajino, G. J. Mathews, and K. Otsuki, Astrophys. J. **554**, 578 (2001).
30 T. A. Thompson, A. Burrows, and B. S. Meyer, Astrophys. J. **562**, 887 (2001).
31 L. F. Roberts, S. E. Woosley, and R. D. Hoffman, Astrophys. J. **722**, 954 (2010).
32 S. E. Woosley, and R. D. Hoffman, Astrophys. J. **395**, 202 (1992).
33 S. Wanajo, Astrophys. J. **770**, L22 (2013).
34 R. I. Epstein, S. A. Colgate, and W. C. Haxton, Phys. Rev. Lett. **61**, 2038 (1988).
35 S. E. Woosley, D. H. Hartmann, R. D. Hoffman, and W. C. Haxton, Astrophys. J. **356**, 272 (1990).
36 P. Banerjee, W. C. Haxton, and Y. Z. Qian, Phys. Rev. Lett. **106**, 201104 (2011).
37 P. Banerjee, Y.-Z. Qian, A. Heger, and W. C. Haxton, EPJ Web. Conf. **109**, 06001 (2016).
38 J. M. Lattimer, F. Mackie, D. G. Ravenhall, and D. N. Schramm, Astrophys. J. **213**, 225 (1977).
39 O. Korobkin, S. Rosswog, A. Arcones, and C. Winteler, Mon. Not. R. Astron. Soc. **426**, 1940 (2012).
40 A. Bauswein, S. Goriely, and H. T. Janka, Astrophys. J. **773**, 78 (2013).
41 O. Just, A. Bauswein, R. A. Pulpillo, S. Goriely, and H. T. Janka, Mon. Not. R. Astron. Soc. **448**, 541 (2015).
42 B. P. Abbott, et al. (LIGO Scientific Collaboration and Virgo Collaboration), Phys. Rev. Lett. **119**, (2017).
43 S. J. Smartt, T. W. Chen, A. Jerkstrand, M. Coughlin, E. Kankare, S. A. Sim, M. Fraser, C. Inserra, K. Maguire, K. C. Chambers, M. E. Huber, T. Krühler, G. Leloudas, M. Magee, L. J. Shingles, K. W. Smith, D. R. Young, J. Tonry, R. Kotak, A. Gal-Yam, J. D. Lyman, D. S. Homan, C. Agliozzo, J. P. Anderson, C. R. Angus, C. Ashall, C. Barbarino, F. E. Bauer, M. Berton, M. T. Botticella, M. Bulla, J. Bulger, G. Cannizzaro, Z. Cano, R. Cartier, A. Cikota, P. Clark, A. De Cia, M. Della Valle, L. Denneau, M. Dennefeld, L. Dessart, G. Dimitriadis, N. Elias-Rosa, R. E. Firth, H. Flewelling, A. Flörs, A. Franckowiak, C. Frohmaier, L. Galbany, S. González-Gaitán, J. Greiner, M. Gromadzki, A. N. Guelbenzu, C. P. Gutiérrez, A. Hamanowicz, L. Hanlon, J. Harmanen, K. E. Heintz, A. Heinze, M. S. Hernandez, S. T. Hodgkin, I. M. Hook, L. Izzo, P. A. James, P. G. Jonker, W. E. Kerzendorf, S. Klose, Z. Kostrzewa-Rutkowska, M. Kowalski, M. Kromer, H. Kuncarayakti, A. Lawrence, T. B. Lowe, E. A. Magnier, I. Manulis, A. Martin-Carrillo, S. Mattila, O. McBrien, A. Müller, J. Nordin, D. ONeill, F. Onori, J. T. Palmerio, A. Pastorello, F. Patat, G. Pignata, P. Podsiadlowski, M. L. Pumo, S. J. Prentice, A. Rau, A. Razza, A. Rest, T. Reynolds, R. Roy, A. J. Ruiter, K. A. Rybicki, L. Salmon, P. Schady, A. S. B. Schultz, T. Schweyer, I. R. Seitenzahl, M. Smith, J. Sollerman, B. Stalder, C. W. Stubbs, M. Sullivan, H. Szegedi, F. Taddia, S. Taubenberger, G. Terreran, B. van Soelen, J. Vos, R. J. Wainscoat, N. A. Walton, C. Waters, H. Weiland, M. Willman, P. Wiseman, D. E. Wright, Wyrzykowski, and O. Yaron, Nature **116**, (2017).
44 D. Kasen, B. Metzger, J. Barnes, E. Quataert, and E. Ramirez-Ruiz, Nature **192**, (2017).